

Interaction of Polyphenylsilsesquioxane With Various β -diketonate Complexes of Titanium By Mechanochemical Activation

Vitaliy V. Libanov

Far Eastern Federal University

Vitaliy Libanov (✉ puly2004@mail.ru)

<https://orcid.org/0000-0001-6135-7159>

Alevtina A Kapustina

Nikolay P Shapkin

Anna Tarabanova

Anna Ryumina

Alexandr A Karabtsov

Valeriy Kuryavyi

Research Article

Keywords: titaniumphenylsiloxanes, mechanochemical synthesis, green chemistry, polyphenylsilsesquioxane, titanium dichloride b-diketonates

Posted Date: February 2nd, 2022

DOI: <https://doi.org/10.21203/rs.3.rs-1308271/v1>

License:   This work is licensed under a Creative Commons Attribution 4.0 International License.

[Read Full License](#)

Abstract

In the present work, we studied the interaction of polyphenylsilsesquioxane with various β -diketonate complexes of titanium by mechanochemical activation. Polyphenylsilsesquioxane, bis-(2,4-pentanedionate) titanium dichloride, bis-(1-phenyl-1,3-butanedionate) titanium dichloride and bis-(1,3-diphenyl-1,3-propanedionate) titanium dichloride were used as starting reagents. Synthesis products were studied by various chemical and physicochemical methods of analysis. The composition of the obtained compounds has been determined. It is shown that under conditions of mechanochemical activation, high molecular weight products with a Si/Ti ratio different from the specified ones are formed. In addition, under the action of mechanical stresses, the initial titanium complexes (with the exception of acetylacetonate) polymerize with the formation of coordination high-molecular compounds, which are destroyed by the addition of ethyl alcohol.

The work is fundamental and contributes to the understanding of the mechanisms of mechanochemical synthesis. The work is aimed at finding effective and environmentally friendly methods for the synthesis and modification of elementorganic high-molecular compounds.

1 Introduction

The method of mechanochemical activation is becoming more and more popular not only in the synthesis of inorganic and organic compounds [1–8], but also in the modification of elementorganic polymers [9–14]. It is widely used as one of the methods for modifying high molecular weight compounds, as well as for processing secondary polyolefins [15], removing persistent organic pollutants [16].

Titansiloxanes are of considerable scientific and practical interest. They are widely used as Ziegler-Natta catalysts [17], catalysts for oxidation and polymerization [18–20], and epoxidation [21, 22]. In addition, they are precursors of materials for medicine and microbiology.

The authors of work [23] used diethoxydimethylsilane and titanium isopropoxide to obtain polymer nanocomposites by the sol-gel process. It was found that, depending on the Ti/Si molar ratio, gels and films (both flexible and brittle) with an average thickness of 20 μm can be obtained, which were subsequently used for laser matrices. The structural model of the gel, proposed by the authors, is a siloxane chain as the basis of a matrix framing titanium dioxide particles. The addition of coumarin 4 and rhodamine 6G to such films gives them optical properties. Titanium dioxide nanoparticles, derivatized by trifunctional siloxanes, exhibit hydrophobic properties (contact angle of about 140–150°), full buoyancy above water, and excellent self-cleaning properties [24].

For the first time the synthesis of high molecular weight titansiloxanes was reported by the authors of work [25]. Andrianov and co-workers found that the cohydrolysis of dimethyldichlorosilane, diethyldichlorosilane and methylphenyldichlorosilane with bis-(acetylacetonate) titanium dichloride in the absence of an acceptor proceeds with the formation of polymers with titanium siloxane bonds. The

authors also showed that 60% of the initial titanium complex polymerizes independently and does not interact with silanes. When carrying out the reaction with pyridine, the yield of titansiloxanes increases to 70%.

There are also a number of difficulties in the synthesis of titanasiloxanes. Thus, the authors of work [26] showed that if in the initial organosilicon compound silicon atom has a tert-butyl group, then a derivative with one or two cyclopentadienyl rings at the metal atom can be obtained, which cannot be done in the case of an ethyl or phenyl substituent at the silicon atom.

The presence of a branched organic group in the silicon atom makes it possible to use in these reactions not only diols, but also organosilanetriols [27]. The fluorenyl group has the greatest screening effect, the use of which makes it possible to exclude the self-condensation of silanetriols during their interaction with titanium alkoxides, leading to the formation of framework titanasiloxanes [28, 29].

Titanasiloxanes can also be obtained by mixing titanium dioxide nanoparticles with a ready-made polymer matrix, as it was done by the authors of works [30–33], by sol-gel synthesis based on titanium alkoxides [34–36]. The processes of direct interaction of titanium alkoxides with hydromethylsiloxane, as well as cleavage of the siloxane bond in the copolymer hydromethylsiloxane-phenylmethylsiloxane under the action of tetrabutyltitanium, have been studied [37].

Titanasiloxanes are formed by the interaction of organotitanium oxides with silanols of various functionality [38]. In this case, the use of tri-functional tert-butylsilanetriol as a starting organosilicon compound at room temperature leads to the formation of intermediate complexes, which upon heating form compounds with an adamantane structure. Gunji [39] synthesized cyclic titanium siloxanes based on organosilicon diols and 2,4-pentanedionate titanium complexes. Pyrolysis of such compounds led to the formation of ceramics consisting of amorphous silicon dioxide and crystalline titanium dioxide.

"Classical" reactions of tri-functional organosilicon compounds with tri-functional organotitanium compounds should lead to the formation of amorphous ladder polymers. However, the use of compounds with bulky organic groups (triphenylmethylsilanthriol and cyclopentadienyltitanium trichloride) in work [40] led to the formation of framework eighteen-membered cyclic compounds. The condensation reactions of silanetriols and titanium alkoxides were also studied in works [41–44]. The authors found out the dependences of the yields and composition of the products on the synthesis temperature, the type and the nature of the solvents, and the nature of organic substituents at the silicon and titanium atoms.

For the synthesis of titanasiloxanes, the so-called exchange decomposition reactions leading to the formation of crystalline low-molecular-weight products were also used [45].

In this work, for the synthesis of titanasiloxanes, we applied a new method based on the mechanochemical interaction of the starting compounds.

2 Experimental

2.1 Materials

In this work, we used commercial solvents, which were purified according to standard methods. The physical constants coincided with the literature data. As starting reagents, we used chemically pure titanium tetrachloride (Eko-tec, Russia), pentane-2,4-dione (Ekos-1, Russia), 1-phenylbutane-1,3-dione (Alfa Aesar, Germany), 1, 3-diphenylpropane-1,3-dione (Alfa Aesar, Germany). Phenyltrichlorosilane was distilled at a temperature of 201-202 ° C.

2.2 Synthesis of starting reagents

2.2.1 Polyphenylsilsesquioxane (PPSSO) was synthesized as it was described previously [14]. The compound with the composition $[C_6H_5SiO_{1.5} \cdot 0.26H_2O]_n$ was obtained with a yield of 94.3%.

Found/calculated, %: Si 20.8/20.9; C 53.8/53.8.

2.2.2 Dichloro-bis-(4-oxopent-2-en-2-olate) titanium (IV) ($L^1_2 TiCl_2$, bis-(acetylacetonato) titanium dichloride) (complex 1). 0.1 mol of titanium tetrachloride was slowly added to a mixture consisting of 50 ml of chloroform, 50 ml of carbon tetrachloride, and a small excess of acetylacetone (from the calculated value). The synthesis was carried out with continuous stirring for two hours. The resulting red precipitate was filtered and dried in a vacuum oven at a temperature of 75°C. Melting temperature 185°C (with decomposition) [46]. Found/calculated, %: C 37.9/37.9, Ti 15.1/15.1, Cl 22.7/22.4.

2.2.2 Dichloro-bis-(3-oxo-1-phenylbut-1-en-1-olate) titanium (IV) ($L^2_2 TiCl_2$, bis-(benzoylacetonato) titanium dichloride) (complex 2). 0.1 mol of titanium tetrachloride was slowly added to a solution of 0.2 mol of 1-phenylbutane-1,3-dione in 50 ml of carbon tetrachloride. The synthesis was carried out with continuous stirring for two hours. The resulting red precipitate was filtered and dried in a vacuum oven at a temperature of 75°C. Melting point 209-210°C (with decomposition) [47]. Found/calculated, %: C 54.5/54.4, Ti 10.8/10.8, Cl 16.3/16.0. 1H NMR ($CDCl_3$, δ): 2.21 (s, 6H, -CH₃), 6.66 (s, 2H, γ -H), 7.39-7.64 (m, 4H, ar), 7.76-7.94 (m, 2H, ar), 7.98 (m, 4H, ar).

2.2.3 Dichloro-bis-(3-oxo-1,3-diphenylprop-1-en-1-olate) titanium (IV) ($L^3_2 TiCl_2$, bis-(dibenzoylmethanato) titanium dichloride) (complex 3). 0.1 mol of titanium tetrachloride was slowly added to a solution of 0.2 mol of 1,3-diphenylpropane-1,3-dione in 50 ml of carbon tetrachloride. The synthesis was carried out with continuous stirring for two hours. The resulting red precipitate was filtered and dried in a vacuum oven at a temperature of 75°C. Melting point is 262-264°C [47]. Found/calculated, %: C 64.0/63.7, Ti 8.5/8.5, Cl 12.9/12.5. 1H NMR ($CDCl_3$, δ): 6.88 (s, 2H, γ -H), 7.32 (m, 6H, ar), 7.48 (m, 8H, ar), 7.57 (m, 2H, ar), 8.01 (m, 4H, ar).

2.3 Reaction of polyphenylsilsesquioxane with titanium dichloride β -diketonates

All the syntheses were carried out in Pulverisette 6 planetary monomill (FRITSCH, Germany). The activating packing was stainless steel balls 0.8 cm in diameter and 4.05 g in weight. The packing weight to payload ratio was approximately 1.8-2. Mechanochemical activation was carried out at a frequency of 600 rpm (10 Hz) for three minutes. Each of the syntheses was carried out in two parallels; the results in

each parallel are reproducible with an accuracy of 0.5% (determined by product yields and results of chemical analysis).

2.3.1 Interaction of polyphenylsilsesquioxane with dichlorobis-(4-oxopent-2-en-2-olate) titanium (IV)

The reactor of the planetary mill was charged with 0.025 mol of polyphenylsilsesquioxane and the same amount of complex 1 (synthesis 1). The initial Si/Ti ratio was 1:1. After activation, the reaction mixture was divided into soluble and insoluble fractions by extraction with toluene in a Soxhlet apparatus. The solvent was distilled off from the soluble fraction. Both fractions were dried in a vacuum oven at a temperature of 75°C. The analysis of the obtained compounds is given in the section Results and Discussions.

2.3.2 Interaction of polyphenylsilsesquioxane with dichlorobis-(3-oxo-1-phenylbut-1-en-1-olate) titanium (IV)

The reactor of the planetary mill was charged with 0.01 mol of polyphenylsilsesquioxane and the same amount of complex 2 (synthesis 2). The initial Si/Ti ratio was 1:1. After activation, the reaction mixture was transferred into a beaker with 100 ml of carbon tetrachloride. The solution was evaporated on a rotary evaporator and dried in a vacuum oven at a temperature of 75°C until constant weight (fraction 1). The insoluble precipitate was additionally treated with chloroform and filtered. After distilling off the solvent and drying in a vacuum oven at a temperature of 75°C, a soluble fraction (fraction 2) and a fraction insoluble in chloroform (fraction 3) were isolated. The analysis of the obtained compounds is given in the section Results and Discussions.

2.3.3 Interaction of polyphenylsilsesquioxane with dichlorobis-(3-oxo-1,3-diphenylprop-1-en-1-olate) titanium (IV)

The reactor of the planetary mill was charged with 0.01 mol of polyphenylsilsesquioxane and the same amount of complex 3 (synthesis 3). The initial Si/Ti ratio was 1:1. The division into fractions was carried out similarly to the previous synthesis. The analysis of the obtained compounds is given in the section Results and Discussions.

2.4 Elemental analysis of the obtained compounds. The determination of silicon was carried out by the gravimetric method [48]. The quantitative determination of titanium was carried out by the method of back titration [49] after the mineralization of polymers with a mixture of concentrated nitric and perchloric acids. Chlorine was determined according to the Schoniger method [50]. Elemental analysis for carbon was carried out on a Flash EA 1112CHN / MAS200 carbon, hydrogen, and nitrogen analyzer (ThermoFinnigan MAT GmbH, USA).

2.5 Gel permeation chromatography. Gel permeation chromatography (GPC) was carried out on a column 980 mm long, 12 mm in diameter, filled with a copolymer of polystyrene and 4% divinylbenzene. The

grain diameter is 0.08-1 mm. Toluene served as the eluent; the flow rate was 1 ml/min. Sample size ~ 0.2 g. Detection was carried out by the gravimetric method according to the content of dry residue in the fractions. A sample of the substance was dissolved in 2 ml of toluene and passed through the column. Fractions of the solution were collected by 3 ml, the solvent was removed in an oven. The column was previously calibrated with substances with different molecular weights: polydimethylsiloxane $\text{H}[\text{Me}_2\text{SiO}]_{30}\text{OH}$ ($M=2238$), octaphenylcyclotetrasiloxane $[\text{Ph}_2\text{SiO}]_4$ ($M=792$), hexaphenylcyclotrisiloxane $[\text{Ph}_2\text{SiO}]_3$ ($M = 594$) and benzoic acid ($M=122$).

2.6 IR spectroscopy. IR spectra were recorded on a Spectrum BX 400 FT-IR spectrometer (Perkin Elmer, USA) in potassium bromide.

2.7 X-ray phase analysis. X-ray phase analysis was performed on a MiniFlex II X-ray diffractometer (RIGAKU, Japan). X-ray tube - Cu, power 0.45 kW, generator power 1 kW, goniometer geometry - vertical, radius - 150 mm, scanning step (2θ) 0.01.

2.8 Nuclear magnetic resonance. NMR spectra were recorded on an Avance 400 MHz high-resolution spectrometer (Bruker, Germany) on ^1H and ^{13}C nuclei at different operating frequencies. Deuterated chloroform and dimethyl sulfoxide- d_6 were used as solvents.

2.9 Scanning electron microscope (SEM). Electron microscopy was carried out using a scanning electron microscope Zeiss EVO 60 (Zeiss, Germany) at various ranges of accelerating voltages.

3 Results And Discussion

The introduction of titanium atoms into the siloxane chain is a difficult task, because titanium compounds have a number of properties that lead to side reactions, such as isomerization of the starting components of the reaction, as well as reactions between the starting materials and the solvent. Mechanochemical activation ensures the elimination of solvents both at the stage of synthesis and (in some cases) at the stage of isolation of reaction products. In our work, we used titanium derivatives in which the atom introduced into the siloxane chain was surrounded by bulky β -diketonate groups. It was assumed that the reaction would proceed according to the schemes [12, 14] previously described by us, and the side processes described in work [25] would be absent due to the exclusion of the solvent in the process of mechanochemical synthesis.

3.1 Synthesis based on dichlorobis-(4-oxopent-2-en-2-olate) titanium (IV)

As a result of the synthesis carried out on the basis of PPSSO and complex 1, two fractions were obtained. The toluene-soluble fraction (fraction 1.1) was a bright orange powder, while the insoluble fraction (fraction 1.2) was a beige powder. The elemental composition of the fractions is shown in Table 1.

Table 1
Data of elemental analysis of products synthesis 1

Fraction	W, %	Found/calculated,%					Yield, %	
		Ti	Si	C	Cl	Si/Ti	Ti	Si
1.1	31.60	(L ₂ TiO)(PhSiO _{1.5}) ₉ (TiO ₂) ₂ (PhSiCl(O))(PhSiO _{0.5} (OH)Cl)						
		7.6/7.5	16.5/16.2	47.6/47.9	3.7/3.7	3.6	18.54	67.58
1.2	68.40	[(L ₂ TiCl ₂) ₅ (TiO ₂) _{0.28}][PhSiO _{1.5} (SiO ₂) _{0.18}]						
		14.9/14.5	1.7/1.9	38.4/38.4	20.3/20.3	1:5.1	78.83	15.37

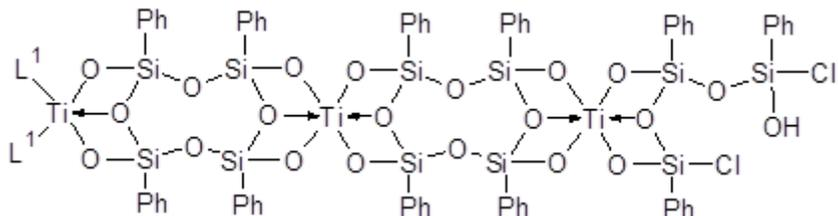
As it can be seen from the data given in Table 1, the obtained Si/Ti ratio in compound 1.1 differed from the specified one and amounted to Si/Ti = 3.6. In the IR spectrum (Fig. 1), there is a broad absorption band in the region of 1000-1028 cm⁻¹, corresponding to vibrations of the siloxane bond. Some shift of the vibrations of the siloxane bond towards lower frequencies indicates the presence of stressed cycles in the macromolecule. The broad absorption band at 1132 cm⁻¹ corresponds to the vibrations of the Si-C^{Ph} bond. The presence of the Ti-O-C bond increases the absorption in the region 1000-1130 cm⁻¹.

Low-intensity vibrations of the bonds of acetylacetonate groups are manifested in the region of 1357 cm⁻¹ (-C-O-Ti), 1527 cm⁻¹ (C=O). Stretching and bending vibrations of CH bonds in the acetylacetonate fragment and phenyl substituent are manifested in the regions of 1430, 3074, 3051, 3008 cm⁻¹; vibrations of the C=C bond in the acetylacetonate fragment are overlapped by the same bonds of the phenyl substituent and are manifested in the 1595 cm⁻¹ region. The broad absorption band at 3431 cm⁻¹ corresponds to free vibrations of the hydroxyl group bound to the silicon atom [51]. Vibrations of the Ti-O bond, which appear as a narrow singlet in the region of 472 cm⁻¹, are overlapped by more intense doublet vibrations of the Si-O bond (497 and 462 cm⁻¹). Noteworthy is the absence of an absorption band in the region of 540 cm⁻¹, which indicates the π-bonding of the carbonyl group of the acetylacetonate fragment with the titanium atom (C=O→Ti) [52]. Vibrations in the 775 cm⁻¹ region correspond to vibrations of the Ti-O bond in an octahedral environment.

According to the data of ¹H NMR spectroscopy, the following signals are present in this compound: a multiplet in the range of 7.13-7.41 ppm. (55 H), corresponding to the chemical shifts of protons in the aromatic ring, two singlets at 5.95 and 5.77 ppm. (2H), corresponding to the chemical shift of protons located in the γ-position of the acetylacetonate ring, singlets at 2.03 and 2.09 ppm. (12H) corresponding to the chemical shifts of the protons of the methyl group of the acetylacetonate ring.

According to the data of gel permeation chromatography, the molecular weight of the obtained compound is about 2000. Whereas compound 1.1 contained reactive functional groups (Si-OH, Si-Cl, and Ti-L¹), we attempted to heat this compound. Upon heating for 20 minutes at 200°C, the absolute weight of the polymer decreased by 8.5%, and the molecular weight increased to 6000. This indicates condensation processes occurring at elevated temperatures, including those associated with the presence

of hydrolytically unstable Si-Cl bonds. In the IR spectra of the polymer obtained upon heating, there were no absorption bands characteristic of the vibrations of the Si-OH and Si-Cl bonds, but acetylacetonate groups were retained. The vibrations of the bonds of the ligand fragment disappeared when the polymer was heated to 300°C, after which the polymer ceased to lose its absolute weight. Thus, the following formula can correspond to compound 1.1:



It was previously shown that the structure of polymetallic organosiloxanes is similar to the structure of layered silicates [example, 53]. The supramolecular structure of such polymers contains ordered regions (lamellas) in which the chains of macromolecules are folded like a ribbon. Such a parameter as the size of the coherent scattering region (CSR), determined by X-ray diffraction analysis can be used to study the supramolecular structure. The CSR corresponds to the size of the lamella in a certain direction, and the first and second reflections on the X-ray diffraction patterns give us the dimensions of the lamella.

It is known [54] that two diffraction maxima appear on the diffraction pattern of polyphenylsilsesquioxane. The first maximum characterizes the interchain distances in the equatorial plane perpendicular to the axes of the macromolecule. The second maximum characterizes mainly intrachain distances of different orientations. In the same work, the authors give an equation for calculating the average diameter of macromolecules (l) according to the position of the first maximum on the intensity distribution curves (the first amorphous halo in the diffractogram):

$$\sqrt{3}l\sin\theta = \lambda$$

In addition to the average diameter of macromolecules, we calculated the size of the coherent scattering region (L) using the Scherrer formula [55], and the cross-sectional area of the macromolecule was calculated using the Miller – Boyer equation [56]. It was shown in work [57] that polyphenylsiloxanes belong to type B according to the Boyer-Miller classification, which corresponds to the coefficients $k_1=0.06$ and $k_2=0.61$ in the equation $\log(d)=k_2\lg(s)+k_1$.

According to X-ray phase analysis data (Table 2,), compound 1.1 is amorphous.

Table 2
Data of X-ray phase analysis of PPSSO and fraction 1.1

Polymer	Reflex		$2\theta(d_1)$, degree	l, nm	D_{CSR} , nm	S, nm ²
	d_1 , nm	d_2 , nm				
PPSSO	1.280	0.4600	8.70	0.13417	2.76	0.8368
1.1	1.140	0.4200	9.10	0.27875	2.70	1.0117

Compared with the initial PPSSO, the interplanar spacing decreases in the fractions under consideration. The decrease in the d_1 value with the introduction of titanium into the siloxane chain is explained by the fact that a coordination bond is formed between the oxygen atoms of one siloxane chain and the vacant d-orbitals of the titanium atom of the neighboring chain. This is also confirmed by the fact that the values of the interplanar spacing increase in polymers with a decrease in the content of titanium atoms in it. Noteworthy are the d_2 values, which are mainly responsible for the intrachain distances. For compound 1.1, this parameter decreases, which indicates the entry of titanium atoms into the interchain space. These conclusions do not contradict IR spectroscopy, which indicates the octahedral environment of the titanium atom.

As for the regions of coherent scattering, there is no dependence on the content of titanium atoms in the polymer. Compared with the initial PPSSO in polymer 1.1, there is a slight decrease in D_{CSR} , which can only indicate a slight increase in internal stresses in crystallites. This is confirmed by the data of electron microscopy of the images (Fig. 2).

According to scanning electron microscopy, the polymer is packed quite tightly. Sample 1.1 contains relatively large agglomerates, as well as macropores. There are no colloidal spheres characteristics of the initial PPSSO [58, 59] in studied compound. We connect with their destruction and fusion as a result of mechanochemical activation.

The average diameter of macromolecules (l) for compound 1.1 significantly increases as compared to the initial PPSSO (more than twofold), indicating that not only the incorporation of a titanium atom into the interchain space, but also the presence of rather bulky acetylacetonate groups at the ends of the polymer chain.

According to the data of elemental and X-ray phase analyzes, IR spectroscopy, the insoluble fraction is compound 1.2, which has the following composition:



Confirmation of the presence in compound 1.2 of PPSSO that did not enter into the reaction is the appearance of an absorption band in the IR spectrum at 1134 cm^{-1} (see Fig. 1 and Fig. 2 in supplementary materials).

In contrast to the results described in work [25], the polymerization of the initial titanium complex under conditions of mechanochemical activation did not occur. However, the yield of polytitanosiloxane was only 31.6%.

3.2 Synthesis based on dichloro-bis-(3-oxo-1-phenylbut-1-en-1-olate) titanium (IV)

We used the benzoylacetate ligand instead of the acetylacetonate ligand to study the effect of the magnitude of the organic ligand of the titanium atom on the ability to cleave the siloxane bond in synthesis 2. In contrast to the previous synthesis, three fractions were isolated after activation: compound 2.1 (yellow), 2.2 (orange), and 2.3 (red). Mass fractions of fractions and elemental analysis are shown in Table 3.

Table 3
Data of elemental analysis of products synthesis 2

Fraction	W, %	Found/calculated,%					Yield, %	
		Ti	Si	C	Cl	Si/Ti	Ti	Si
2.1	21.17	(PhSiO _{1.5}) ₄₁ (PhSiO(OH)) ₁₃ (TiO ₂) ₆ (TiOCl ₂) ₄ 5LH						
		5.0/5.3	16.9/17.0	48.3/50.4	3.1/3.1	5.7	12.43	71.82
2.2	41.82	[(PhSiO _{1.5}) ₂ (OTiL ₂) _n ·4L ₂ TiCl ₂ ·3.5LH						
		7.7/7.9	1.9/1.9	58.8/58.3	9.4/9.4	1:2.4	37.80	17.62
2.3	37.01	10.8(L ₂ TiCl ₂) _n SiO ₂						
		10.7/10.7	0.6/0.6	53.4/53.7	15.2/15.9	1:10.8	46.56	4.46

According to the elemental analysis data, the obtained Si/Ti ratio differs from the specified one and is 5.7:1 for the high-molecular fraction 2.1. In the IR spectrum (Fig. 3), there is a broad absorption band in the region of 1000-1030 cm⁻¹, corresponding to vibrations of the siloxane bond and merging into a doublet with an intense absorption band of the Si-C bond (1132 cm⁻¹). The presence of the Ti-O-C bond also increases the absorption in the 1000-1130 cm⁻¹ region. Vibrations of the Ti-O- bond (in contrast to the analogous product of the previous synthesis) cannot be unambiguously identified by the singlet signal in the 1260 cm⁻¹ region, as it is overlapped by the broadened absorption band of the phenylsiloxane bond and remains in the spectrum as a small shoulder. Low-intensity vibrations of the bonds of benzoylacetate groups appear in the range of 1357 cm⁻¹ (-C-O-Ti), 1488 and 1523 cm⁻¹ (C=O).

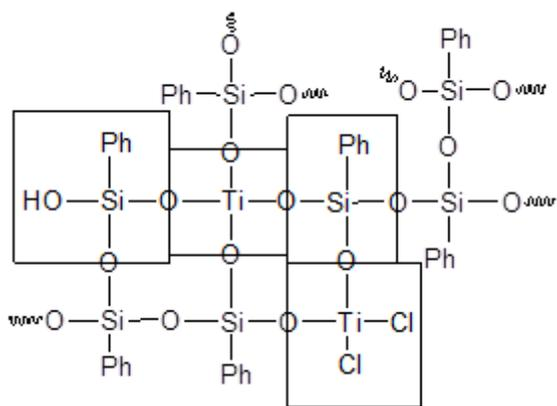
Stretching and bending vibrations of CH bonds in the ligand and phenyl substituent are manifested in the regions of 1431, 3074, 3051, 3008 cm⁻¹; vibrations of the C=C bond in the acetylacetonate fragment are

overlapped by the same bonds of the phenyl substituent and are manifested in the 1595 cm^{-1} region. Noteworthy is the presence of an absorption band in the region of 3631 cm^{-1} , which corresponds to the vibrations of free silanol groups [60]. The vibrations of silanol groups can also be identified by the presence of an absorption band at 852 cm^{-1} . More intense doublet vibrations of the Si-O bond ($497\text{-}447\text{ cm}^{-1}$) overlap vibrations of the Ti-O bond, which appear as a narrow singlet in the region of 472 cm^{-1} . As in the IR spectrum of the previous synthesis, there are no absorption bands in the region of 540 cm^{-1} ($\text{C=O}\rightarrow\text{Ti}$).

In the ^1H NMR spectrum, a signal of low intensity is observed at 6.24 ppm, which corresponds to the proton of the β -diketonate ring in the γ -position, as well as a signal tripled in intensity in the region of 2.26 ppm, corresponding to the chemical shifts of the protons of the methyl group. Broadened multiplet in the range 7.1-7.95 ppm corresponds to chemical shifts of protons in the aromatic ring of both the siloxane and the complex.

The molecular weight of the obtained compound is more than 7000 (the limit of the separability of the chromatographic column). Whereas the data of gel permeation chromatography and NMR spectroscopy did not allow us to determine the molecular weight of the polymer with sufficient approximation, we acylated product 2.1 and titrated the resulting water by the Fisher method. The mass fraction of hydroxyl (silanol) groups was 2.5%. Calculation of the molecular weight based on the content of hydroxyl groups showed that compound 2.1 has a molecular weight of approximately 8900.

High-molecular compound 2.1 contains the following structural units (highlighted in squares):



General composition of the compound 2.1 taking into account the value of the average molecular weight corresponds to the following formula:



While heating the connection 2.1 within 20 minutes at 200°C , the absolute weight of the polymer decreased by 5.0%. This indicates insignificant polymerization processes associated with the presence of silanol groups in the polymer. Further heating did not lead to a loss of absolute mass.

Thus, in the result of mechanochemical activation, not only hydrolysis of the initial complex occurred, due to the content of associated water in PPSSO, but also the abstraction of the ligand. The high chlorine content is due to the presence of surviving fragments of the titanium complex in the chain.

According to X-ray phase analysis data (Table 4, Fig. 3 in supplementary materials), fraction 2.1 is amorphous.

Table 4
Data of X-ray phase analysis of PPSSO and fraction 2.1

Polymer	Reflex		$2\theta(d_1)$, degree	l, nm	D_{CSR} , nm	S, nm ²
	d_1 , nm	d_2 , nm				
PPSSO	1.280	0.4600	8.70	0.13417	2.76	0.8368
2.1	1.239	0.4657	7.12	0.19797	4.04	0.8826

As for the regions of coherent scattering, there is no dependence on the content of titanium atoms in the polymer. Compared with the initial PPSSO in the case of polymer 2.1 these values increase rather strongly, which indicates the improvement of metastable lamellas. This is confirmed by the data of electron microscopy of the images (Fig. 4).

Compared with the initial PPSSO, the interplanar spacing decreases in the fraction under consideration. The decrease in the d_1 value with the introduction of titanium into the siloxane chain is explained by the fact that a coordination bond is formed between the oxygen atoms of one siloxane chain and the vacant d-orbitals of the titanium atom of the neighboring chain. This is also confirmed by the fact that the values of the interplanar spacing increase in polymers with a decrease in the content of titanium atoms in it. Noteworthy are the d_2 values, which are mainly responsible for the intrachain distances. In compound 2.1, this value increases in comparison with the initial PPSSO, which can be explained by the incorporation of a titanium atom into the polymer chain. These conclusions do not contradict IR spectroscopy, which indicates the octahedral environment of the titanium atom.

According to scanning electron microscopy, the polymers are packed quite tightly. Sample 2.1 lack macropores and agglomerates. In polymer 2.1, relatively regular and dense aggregates are formed, the formation of a layered structure can be observed. There are no colloidal spheres characteristics of the initial PPSSO in fraction 2.1. We connect with their destruction and fusion as a result of mechanochemical activation.

For compound 2.1, the average macromolecule diameter increases in comparison with PPSSO by 47%, this may also indicate the partial binding of two neighboring silsesquioxane chains through the titanium atom.

According to the data of elemental analysis (Table 3), IR and NMR spectroscopy (Fig. 4 and Fig. 5 in supplementary materials), XRD (Fig. 5) fraction 2.2 is a mixture consisting of polymeric titansiloxane, a coordination polymer, and a starting ligand. General formula of the mixture:

$[(\text{PhSiO}_{1.5})_2(\text{OTiL}_2)]_n \cdot 4\text{L}_2\text{TiCl}_2 \cdot 3.5\text{LH}$. During gel chromatographic separation of this fraction, the following compounds were isolated separately: polymer titansiloxane $[(\text{PhSiO}_{1.5})_2(\text{OTiL}_2)]_n$ ($M > 6000$, found/calculated, %: Ti 7.4/7.4, Si 8.6/8.7, C 57.9/59.5), coordination oligomer $[\text{L}_2\text{TiCl}_2]_4$ ($M \approx 1800$, found/calculated, %: Ti 10.7/10.8, Si 0.0/0.0, C 54.7/54.4, Cl 16.0/16.1). Benzoylacetone was not isolated and analyzed separately. The isolated tetramer of the starting complex was destroyed by heating in ethyl alcohol to a monomer.

The second high molecular weight fraction was observed in a significant amount only for syntheses 2 and 3. Their amorphous state is confirmed by the data of X-ray phase analysis (Fig. 5). In contrast to the previous fraction, for compound 2.2, the appearance of four halos is observed (Table 5). According to the theory of X-ray diffraction analysis ($\sin^2\theta_{002} = 4\sin^2\theta_{001}$, $\sin^2\theta_{003} = 9\sin^2\theta_{001}$, $\sin^2\theta_{004} = 16\sin^2\theta_{001}$) amorphous halos of the second, third and fourth orders should be located in the angular ranges of diffraction angles $2\theta = 22.34^\circ$, 33.53° , and 44.72° . Thus, the diffraction pattern of compound 2.2 exhibit amorphous halos of the second, third, and fourth orders.

By the presence of additional halos, it can be noted that the presented fractions are not only in an amorphous state, but also in have a certain degree of ordering.

Table 5
Data of X-ray phase analysis of PPSSO and fractions 2.2

Polymer	Reflex								D_{CSR} , nm
	1		2		3		4		
	d, nm	2θ , deg	d, nm	2θ , deg	d, nm	2θ , deg	d, nm	2θ , deg	
PPSSO	1.280	8.70	0.460	19.18	-	-	-	-	2.76
2.2	0.7907	11.18	0.461	19.23	0.342	26.00	0.206	43.90	1.76

It is inappropriate to carry out a comparative analysis of the X-ray diffraction patterns of the obtained compounds with PPSSO, as the fractions are mixtures of polymeric titanium phenylsiloxanes and polymerized coordination complexes. However, the analysis of diffraction patterns showed the presence in the mixture, in addition to the polymer product, of initial complexes in oligomeric states, which confirms the corresponding conclusions made earlier. The amorphization of the initial complexes, as well as the broadening of the diffraction maxima, are primarily associated with microdistortions in crystals, a decrease in crystallites, and the formation of oligomeric products and agglomerates. In Figure 5, the diffraction maxima obtained because of the experiment are highlighted in blue, and the diffraction patterns of the initial titanium complexes are highlighted in red.

These conclusions are also confirmed by the data of electron microscopy. Fig. 6 shows that because of mechanochemical activation, a fraction with is formed agglomerates of a porous structure of various shapes and sizes. Fraction 3.2 has a more ordered structure, which we can observe both on the X-ray (Fig. 5), as well as on the micrograph (Fig. 6).

The presented data of electron microscopy and X-ray phase analysis correlate well with each other. In addition, the size of the coherent scattering region for fraction 2.2 is more than 50% lower than that for the initial PPSSO.

According to the data of elemental and X-ray phase analyzes (Fig. 6 and Table 1 in supplementary materials), IR spectroscopy, the insoluble fraction (2.3) is the initial titanium complex with a small content of silicon oxide: $10.8(L_2TiCl_2) \cdot SiO_2$.

3.3 Synthesis based on dichloro-bis-(3-oxo-1,3-diphenylprop-1-en-1-olate) titanium (IV)

In synthesis 3, we used a titanium complex with more sterically hindered ligand dibenzoylmethanate.

After mechanochemical activation, three fractions were isolated: a yellow high molecular weight fraction (3.1), an orange-red high molecular weight fraction (3.2), and a red low molecular weight fraction (3.3). Elemental analysis of the fractions is shown in Table 6.

Table 6
Data of elemental analysis of products synthesis 3

Fraction	W, %	Found/calculated,%					Yield, %	
		Ti	Si	C	Cl	Si/Ti	Ti	Si
3.1	22.77	[(PhSiO _{1.5}) _{5.2} (PhSiO(OH)) _{1.1} (TiO ₂) _{0.9} (OTiL ₂) _{0.1} 0.3LH] _n						
		4.7/4.7	17.3/17.3	52.8/53.5	-	6.3	11.80	74.14
3.2	53.90	[(PhSiO _{1.5})(OTiL ₂) _{0.9} (TiO ₂)] _n ·1.9(L ₂ TiCl ₂)						
		10.4/10.4	1.6/1.6	62.2/62.0	7.9/7.7	1:3.8	61.79	16.23
3.3	23.33	L ₂ TiCl ₂ 0.06SiO ₂ 0.9H ₂ O						
		8.2/8.2	0.3/0.3	60.0/61.4	12.2/12.1	1:16	21.10	1.32

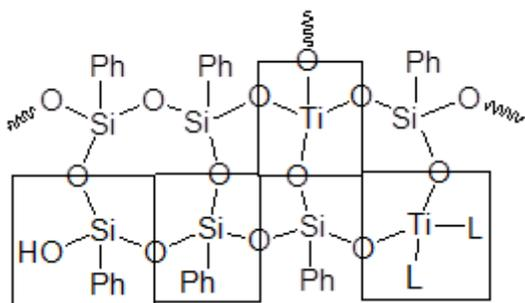
According to the elemental analysis data, the obtained Si/Ti ratio differs from the specified one and is equal to 6.3. In contrast to the previous synthesis, there is no chlorine in the analogous high molecular weight fraction 3.1. In addition, according to IR spectroscopy data (see Fig. 7), there is a small amount of diketonate groups, both free and bound to titanium (1554 and 1521 cm⁻¹).

In addition, in the IR spectrum, vibrations of bonds of hydroxyl groups (3631 and 854 cm^{-1}) and associated water (3406 cm^{-1}) are observed; an intense absorption band in the region of 1028 cm^{-1} , characteristic of antisymmetric vibrational vibrations of the siloxane bond. Signals in the range of 3008 , 3051 , 3072 , 2920 , 1597 , 1431 , 1132 , and 696 cm^{-1} correspond to bond vibrations in phenyl substituents and Si-Ph (Si-C, C=C, C-H). The Ti-L bond can be identified by the vibration in the 1355 cm^{-1} region, and the Si-O-Ti bond at 920 cm^{-1} , which is overlapped by an intense absorption band of the siloxane bond and is observed in the spectrum as a small shoulder.

The average molecular weight of compound 3.1, according to gel permeation chromatography data, exceeds the column divisibility limit and is more than 6000. Heating to 200°C did not lead to a noticeable weight loss (less than 2%), which allows us to conclude that there are insignificant condensation processes, including the absence of chlorine atoms in the polymer.

The NMR spectrum on the proton nuclei confirms the insignificant content of diketonate groups (a weak and low-intensity signal in the region of 6.43 ppm, corresponding to the proton in the γ -position of the diketonate ring).

Based on GPC, elemental analysis, IR and NMR spectroscopy, it can be concluded that the high molecular weight fraction 3.1 corresponds to the compound of general formula $[(\text{PhSiO}_{1.5})_{5.2}(\text{PhSiO}(\text{OH}))_{1.1}(\text{TiO}_2)_{0.9}(\text{OTiL}_2)_{0.1} 0.3\text{LH}]_n$. Structurally, the elements of compound 3.1 can be depicted as follows:



According to X-ray phase analysis data (Table 4, Fig. 7 in supplementary materials), fraction 3.1 is amorphous.

Table 7
Data of X-ray phase analysis of PPSSO and fraction 3.1

Polymer	Reflex		$2\theta(d_1)$, degree	l, nm	D_{CSR} , nm	S, nm^2
	d_1 , nm	d_2 , nm				
PPSSO	1.280	0.4600	8.70	0.13417	2.76	0.8368
3.1	1.244	0.4622	7.10	0.12202	3.87	0.8768

Compared with the initial PPSSO, the interplanar spacing decreases in the fractions under consideration. The decrease in the d_1 value with the introduction of titanium into the siloxane chain is explained by the fact that a coordination bond is formed between the oxygen atoms of one siloxane chain and the vacant d-orbitals of the titanium atom of the neighboring chain. This is also confirmed by the fact that the values of the interplanar spacing increase in polymers with a decrease in the content of titanium atoms in it. Noteworthy are the d_2 values, which are mainly responsible for the intrachain distances. In compound 3.1, this value increases in comparison with the initial PPSSO, which can be explained by the incorporation of a titanium atom into the polymer chain. These conclusions do not contradict IR spectroscopy, which indicates the octahedral environment of the titanium atom.

Compared with the initial PPSS, in polymer 3.1, there is a slight increase in D_{CSR} , which can only indicate a slight decrease in internal stresses in crystallites. In the cases of polymer 3.1, these values increase rather strongly, which indicates the improvement of metastable lamellas. This is confirmed by the data of electron microscopy of the images (Fig. 8).

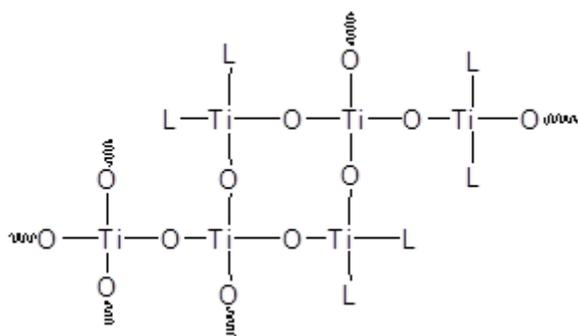
Sample 3.2 lack macropores and agglomerates. In polymer 2.1 (Fig. 4), relatively regular and dense aggregates are formed, while in polymer 3.1 (Fig. 8), the formation of a layered structure can be observed. There are no colloidal spheres characteristics of the initial PPSSO in all three studied compounds. We connect with their destruction and fusion as a result of mechanochemical activation.

In compound 3.1, the average diameter of the macromolecule becomes smaller due to the lower content of ligands at the titanium atom, this makes possible the "constriction" of polymer chains due to the donor-acceptor interaction.

As in synthesis 2, in the result of mechanochemical activation, fraction 3.2 was isolated, which is a mixture of polytitanphenylsiloxane and the initial complex (Fig. 8 and Fig. 9 in supplementary materials). General formula of the mixture: $[(\text{PhSiO}_{1.5})(\text{OTiL}_2)_{0.9}(\text{TiO}_2)]_n \cdot 1.9(\text{L}_2\text{TiCl}_2)$. The mixture was separated using GPC. A polymer with the composition $[(\text{PhSiO}_{1.5})(\text{OTiL}_2)_{0.9}(\text{TiO}_2)]_n$ and a titanium complex were isolated. However, in contrast to the previous synthesis, the high molecular weight compound was not polytitanphenylsiloxane, but it was a mixture consisting of polyphenylsiloxane and a polymer titanium complex. This was determined by dissolving this fraction in toluene: polyphenylsiloxane went into solution, and the polymer titanium complex was filtered off. Thus, fraction 3.2 was divided into three compounds: $[\text{PhSiO}_{1.5} \cdot 0.07\text{H}_2\text{O}]_n$ ($m=0.2094$ g, $M>6000$, found/calculated, %: Si 21.5/21.5, C 54.7/55.3); $[(\text{L}_2\text{TiO})_{0.9}(\text{TiO}_2)]_n$ ($m=0.9069$ g, $M>6000$, found/calculated, %: Ti 17.1/16.9, C 61.1/60.1); L_2TiCl_2 ($m=1.7237$ g, $M=565$, found/calculated, %: Ti 8.1/8.5, C 63.6/63.7, Cl 13.0/12.6).

In the IR spectrum of the polymerized titanium complex, vibrations of the bonds of the phenyl substituents of the dibenzoylacetate ligand ($2862, 2925, 2974, 1593 \text{ cm}^{-1}$), the C=C and C=O bonds of the diketone (1517 and 1487 cm^{-1}) are observed. The vibrations of the Ti-O bond bound to the ligand are manifested in the region of 1350 cm^{-1} , and the titanoxane bond (Ti-O-Ti) in the region of 771 cm^{-1} , due to the symmetric stretching vibrations of the Ti-O bonds of the TiO_4 tetrahedron [61]. X-ray phase

analysis confirms the polymeric character of this fraction. It is assumed that the polymerized titanium complex has the following cycloliner structure:



The second high molecular weight fraction is observed in a significant amount only for syntheses 2 and 3. Their amorphous state is confirmed by the data of X-ray phase analysis (Fig. 9). In contrast to the previous fractions, for compound 3.2, the appearance of four halos is observed (Table 8). Thus, the diffraction pattern of compound 3.2 exhibit amorphous halos of the second, third, and fourth orders. By the presence of additional halos, it can be noted that the presented fractions are not only in an amorphous state, but also in have a certain degree of ordering.

Table 8
Data of X-ray phase analysis of PPSSO and fractions 3.2

Polymer	Reflex								D_{CSR} , nm
	1		2		3		4		
	d, nm	2θ , deg	d, nm	2θ , deg	d, nm	2θ , deg	d, nm	2θ , deg	
PPSSO	1.280	8.70	0.460	19.18	-	-	-	-	2.76
3.2	1.0200	8.66	0.479	18.50	0.343	25.95	0.205	44.17	3.29

It is inappropriate to carry out a comparative analysis of the X-ray diffraction patterns of the obtained compounds with PPSSO, as the fractions are mixtures of polymeric titanium phenylsiloxanes and polymerized coordination complexes. However, the analysis of diffraction patterns showed the presence in the mixture, in addition to the polymer product, of initial complexes in oligomeric states, which confirms the corresponding conclusions. The amorphization of the initial complexes, as well as the broadening of the diffraction maxima, are primarily associated with microdistortions in crystals, a decrease in crystallites, and the formation of oligomeric products and agglomerates. In Fig. 9, the diffraction maxima obtained because of the experiment are highlighted in blue, and the diffraction patterns of the initial titanium complexes are highlighted in red.

These conclusions are also confirmed by the data of electron microscopy. Fig. 10 shows that because of mechanochemical activation, a fraction with is formed agglomerates of a porous structure of various

shapes and sizes. Fraction 3.2 has a more ordered structure, which we can observe both on the X-ray (Fig. 8), as well as on the micrograph (Figure 9). As can be seen from the results of scanning electron microscopy, there are no agglomerates, spherical formations, and colloidal spheres capable of further coalescence in fraction 3.2. The structure of the joint is uniform, but there are many microcracks.

The presented data of electron microscopy and X-ray phase analysis correlate well with each other. In addition, the size of the coherent scattering region for fraction 3.2, the opposite picture is observed: the CSR size increases with increasing ordering in the structure.

According to the data of elemental and X-ray phase (Fig. 10 and Table 2 in additional materials) analyzes, IR and NMR spectroscopy, the insoluble fraction (3.3) is the initial titanium complex with an insignificant content of hydrated silicon oxide: $L_2TiCl_2 \cdot 0.06SiO_2 \cdot 0.9H_2O$.

4 Conclusions

Based on the work done, the possibility of synthesizing polytitanophenylsiloxanes was shown. It was found that under conditions of mechanochemical activation, high molecular weight products with a Si/Ti ratio differing from the specified ones are formed. In this case, the resulting ratios increase with an increase in the size of the ligand of the titanium atom due to the smaller incorporation of titanium into the polymer chain. It was shown that under the conditions of mechanochemical activation in the case of the benzoylacetate complex, an oligomeric product is formed, which is a coordination tetramer. In the case of using titanium dichloride dibenzoylmethanate as the initial complex, under the conditions of mechanochemical activation, a significant part of it undergoes decomposition with the formation of its own polymer product.

References

1. Z. Li, M. Chen, Q. Zhang, D. Tao, *Journal of Alloys and Compounds*. 845, 156291 (2020)
2. K. Jie, Y. Zhou, Q. Sun, B. Li, R. Zhao, D. Jiang, W. Guo, H. Chen, Z. Yang, F. Huang, S. Dai, *Nature Communications*. 11, 1086 (2020)
3. N.V. Bulina, M.V. Chaikina, I.Yu. Prosanov, D.V. Dudina, *Materials Science and Engineering: B*. 262, 114719 (2020)
4. S. Liu, B. Li, Y. Wu, K. Luo, Z. Zhao, Y. Zhang, *Journal of The American Ceramic Society*. 103 (11), 6112 (2020)
5. L.S. Germann, M. Arhangelskis, M. Etter, R.E. Dinnebier, T. Frišćić, *Chem. Sci*. 11, 10092 (2020)
6. A.S. Al-Bogami, T.S. Saleh, A.H. Al-Shareef, *J. Heterocyclic Chem*. 57 (10), 3605 (2020)
7. T. Feiler, B. Bhattacharya, A.A.L. Michalchuk, V. Schröder, E. List-Kratochvil, F. Emmerling, *Crystals* 10 (10), 889 (2020)
8. Y. Liu, M. Hou, Y. Yang, X. Duan, L. He, D. Yang, *ACS Sustainable Chem. Eng*. 8 (32), 11940 (2020)
9. A.A. Kapustina, N.P. Shapkin, E.B. Ivanova, A.A. Lyakhina, *Russ. J. Gen. Chem*. 75, 571 (2005)

10. N.P. Shapkin, A.A. Kapustina, E.A. Talashkevich, *Russ. J. Inorganic Chem.* 45 (4), 601 (2000)
11. N.P. Shapkin, A.A. Kapustina, N.V. Dombai, V.V. Libanov, I.G. Khalchenko, S.V. Gardionov, V.V. Gribova, *Polym. Bull.* 77, 1177 (2020)
12. V.V. Libanov, A.A. Kapustina, N.P. Shapkin, A.A. Rumina, *Silicon* 11 (3), 1489 (2019)
13. N.P. Shapkin, A.A. Kapustina, S.V. Gardionov, I.G. Khal'chenko, V.V. Libanov, E.A. Tokar, *Silicon* 11 (5), 2261 (2019)
14. V. Libanov, A. Kapustina, N. Shapkin, P. Dmitrinok, Z. Puzyrkov, *Polymer* 194, 122367 (2020)
15. S. Yin, R. Tuladhar, F. Shi, R.A. Shanks, M. Combe, T. Collister, *Polymer Engineering and Science* 55 (12), 2899 (2015)
16. G. Cagnetta, J. Huang, B. Wang, S. Deng, G. Yu, *Chemical Engineering Journal* 291 30 (2016)
17. Jia-Chu Liu, *Appl. Organometal. Chem.* 13, 295 (1999).
18. V. Lorenz, A. Fischer, S. Giessmann, J.W. Gilje, Y. Gun'ko, K. Jacob, F.T. Edelmann, *Coordination Chemistry Reviews* 206-207, 321 (2000)
19. M. Mateos, J. Vinueza, M. E.G. Mosquera, V. Tabernerero, T. Cuenca, G. Jiménez, *Inorganica Chimica Acta* 501, 119275 (2020)
20. D. Agrawal, S.K. De, P.K. Singh, *J Polym Res* 27, 99 (2020)
21. T. Maschmeyer, M.C. Klunduk, C.M. Martin, D.S. Shephard, J.M. Thomas, B.F.G. Johnson, *Chem. Commun.* 19, 1847 (1997)
22. M.Ventura, M.E.G. Mosquera, T. Cuenca, B. Royo, G. Jimenez, *Inorg. Chem.* 51, 6345 (2012)
23. S. Dire, F. Babonneau, G. Carturan, J. Livage, *Journal of Non-Crystalline Solids.* 147-148, 62 (1992)
24. F. Milanese, G. Cappelletti, R. Annunziata, C.L. Bianchi, D. Meroni, S. Ardizzone, *J. Phys. Chem. C* 114 (18), 8287 (2010)
25. K.A. Andrianov, Sh.V. Pichkhadze, I.V. Bochkareva, *Polyorganotitanosiloxanes. Journal of Polymer Science* 3(9), 1321 (1961) [in Russia]
26. F.-Q. Liu, I. Uson, H.W. Roesky, *J. Chem. Soc. Dalton Trans.* 2453 (1995)
27. A. Voigt, R. Murugavel, H.W. Roesky, H.-G. Schmidt, *Journal of Molecular Structure*, 436-437, 49 (1997)
28. H.M. Lindemann, M. Schneider, B. Neumann, H.-G. Stammler, A. Stammler, P. Jutzi, *Organometallics* 21(14), 3009 (2002)
29. J.-O. Nolte, M. Schneider, B. Neumann, H.-G. Stammler, P. Jutzi, *Organometallics* 22(5), 1010 (2003)
30. W. Liao, S. Hsiao, Y. Wu, S. Zeng, S. Li, Y. Wang, C. Ma, *RSC Adv.* 4, 38614 (2014)
31. K. Lem, D. Nguyen, H. Kim, D. Lee, *Journal of Nanoscience and Nanotechnology*, 11(8), 7202 (2011)
32. M. Kuo, S. Chang, P. Hsieh, Y. Huang, C. Li, *J. Amer. Ceram. Soc.* 99(2), 445 (2016)
33. T. Yang, S. Chang, C. Li, P. Huang, *J. Amer. Ceram. Soc.* 100, 56 (2017)
34. I. Lei, D. Lai, T. Don, W. Chen, Y. Yu, W. Chiu, *Mater. Chem. Phys.* 144 (1-2), 41 (2014)
35. Y. Lai, L. Jin, J. Hang, X. Sun, L. Shi, *J. Coat. Technol. Res.* 12, 1185 (2015)

36. X. Luo, C. Zha, B. Luther-Davies, J. Sol-Gel. Sci. Technol. 32, 297 (2004)
37. S. Rubinsztajn, J. Chojnowski, M. Cypryk, U. Mizerska, P. Uznanski, A. Walkiewicz-Pietrzykowska, Appl Organometal. Chem. 34:e5571 (2020)
38. J.J. Carbo, O.G. Moral, A. Martin, M. Mena, J.-M. Poblet, C. Santamaria, Chemistry A European Journal 14 (26), 7930 (2008)
39. T. Gunji, K. Kubota, S. Kishiki, Y. Abe, Bulletin of the Chemical Society of Japan 75 (3), 537 (2002)
40. J.H. Kim, S.H. Kang, I.N. Jung, B.R. Yoo, M.E. Lee, J. Sol-Gel Sci. Technol. 32, 31 (2004)
41. H.M. Lindemann, M. Schneider, B. Neumann, H.-G. Stammer, A. Stammer, P. Jutzi, Organometallics 21 (14), 3009 (2002)
42. P. Jutzi, H.M. Lindemann, J.-O. Nolte, M. Schneider, Silicon Chemistry: From the Atom to Extended Systems, p. 372-382 (2003)
43. J.-O. Nolte, M. Schneider, B. Neumann, H.-G. Stammer, P. Jutzi, Organometallics 22 (5), 1010 (2003)
44. A. Voigt, R. Murugavel, V. Chandrasekhar, N. Winkhofer, H.W. Roesky, H.-G. Schmidt, I. Uson, Organometallics 15 (6), 1610 (1996)
45. R. Murugavel, V.S. Shete, K. Baheti, P. Davis, Journal of Organometallic Chemistry 625 (2), 195 (2001)
46. Y. Kawasaki, T. Tanaka, R. Okawara, Bulletin of the Chemical Society of Japan, 40 (7), 1562 (1967)
47. N. Serpone, R.C. Fay, Inorganic Chemistry, 6 (10), 1835 (1967)
48. J.A. McHard, P.C. Servais, H.A. Clark, Anal. Chem. 20 (4), 325 (1948)
49. H.J. Marini, R.I. Anton, R.A. Olsina, Talanta, 37 (11), 1097 (1990)
50. W. Schöniger, Mikrochim Acta, 44, 869 (1956)
51. B. Arkles, G.L. Larson (eds.), Silicon Compounds: Silanes & Silicones, Gelest, Inc., Morrisville, PA, USA, third edition (2013), 610 p. ISBN 978-0-578-12235-9.
52. D.C. Bradley, C.E. Holloway, J. Chem. Soc. (A), 282 (1969)
53. M.G. Voronkov, N.P. Shapkin, J Organomet. Chem., 389 (2), 169 (1990)
54. D.Ya. Tsvankin, V.Yu. Levin, V.S. Pankov, V.P. Zhukov, A.A. Zhdanov, K.A. Andrianov, Polymer Science U.S.S.R., 21 (9), 2348 (1979)
55. P. Scherrer, Bestimmung der inneren Struktur und der Größe von Kolloidteilchen mittels Röntgenstrahlen. In: Kolloidchemie Ein Lehrbuch. Chemische Technologie in Einzeldarstellungen (1912). Springer, Berlin, Heidelberg.
56. R.L. Miller, R.F. Boyer, Journal of Polymer Science: Polymer Physics Edition, 22 (12), 2043 (1984)
57. N.P. Shapkin, Yu.N. Kulchin, V.I. Razov, S.S. Voznesenskii, V.V. Bazhenov, M.V. Tutov, N.N. Stavnisty, V.G. Kuryavyi, Russian Chemical Bulletin, 60 (8), 1640 (2011)
58. W. Maa, D. Zhang, Yu Duan, H. Wang, J Colloid and Interface Science, 392,194 (2013)
59. L.A.S.D.A. Prado, E. Radovanovic, H.O. Pastore, I.V.P. Yoshida, J Polymer Science, Part A: Polymer Chemistry, 38 (9), 1580 (2000)

60. G.D. Chukin, J. Appl. Spectrosc, 8, 527 (1968)

61. A.N. Murashkevich, A.S. Lavitskaya, T.I. Barannikova, I.M. Zharskii, J. Appl. Spectrosc, 75, 730 (2008)

Figures

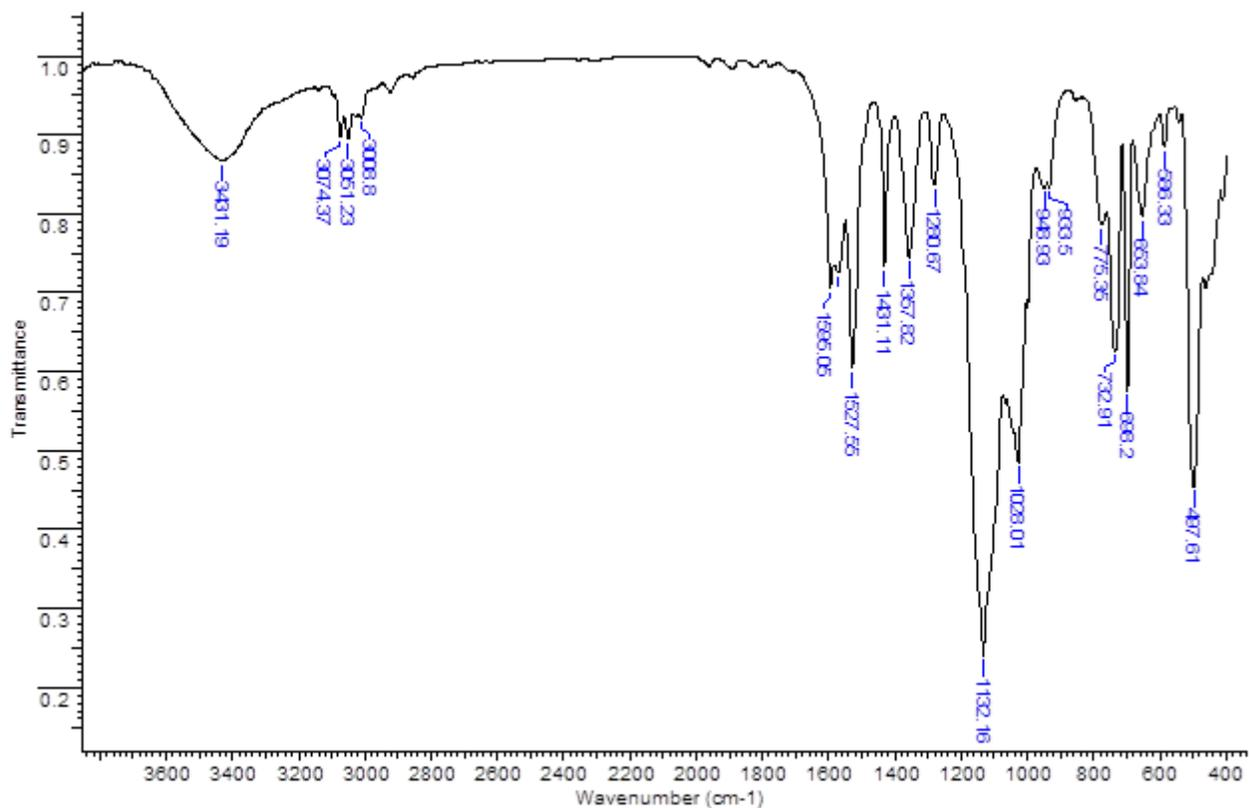


Figure 1

FT-IR spectra of fraction 1.1

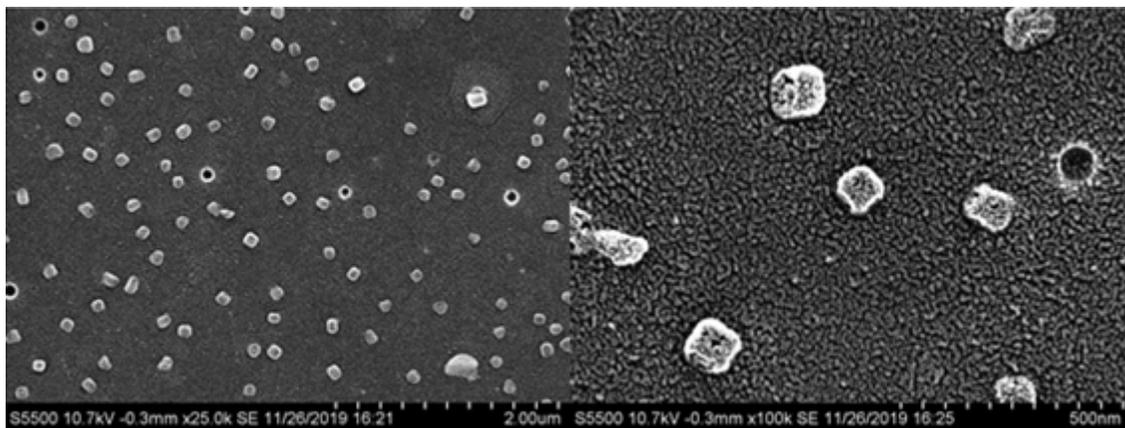


Figure 2

Scanning electron microscopy of the sample 1.1

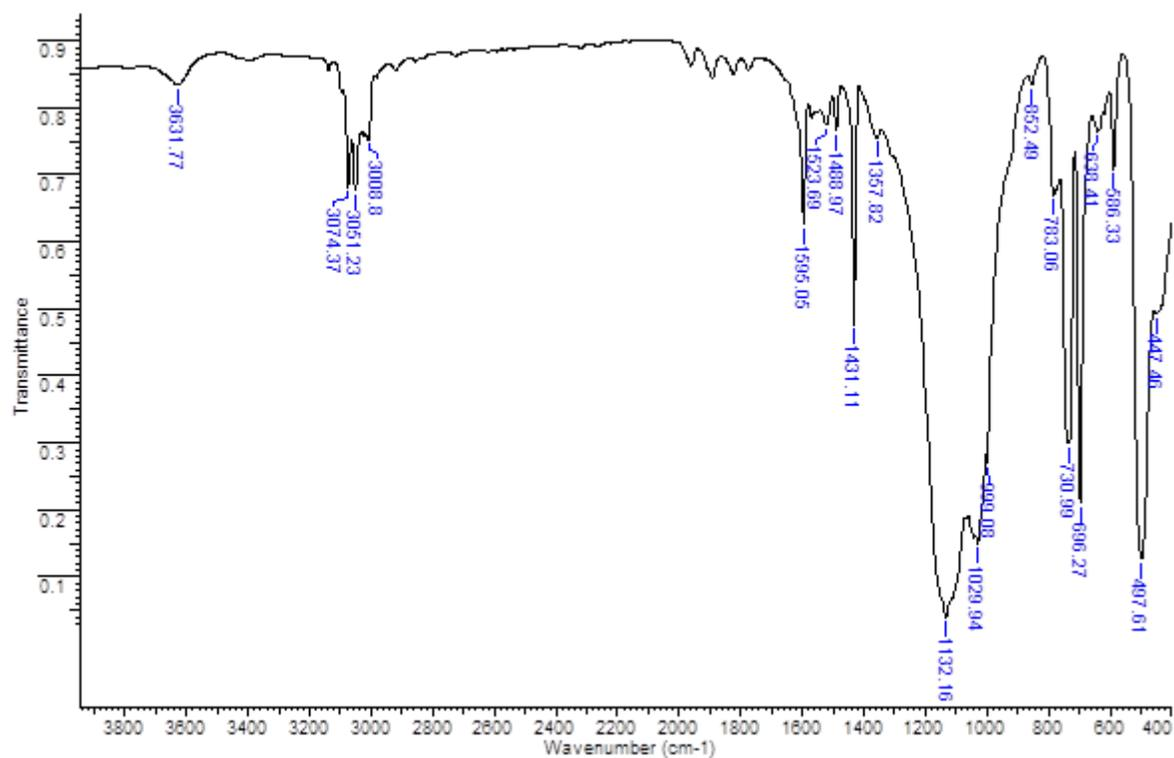


Figure 3

FT-IR spectra of fraction 2.1

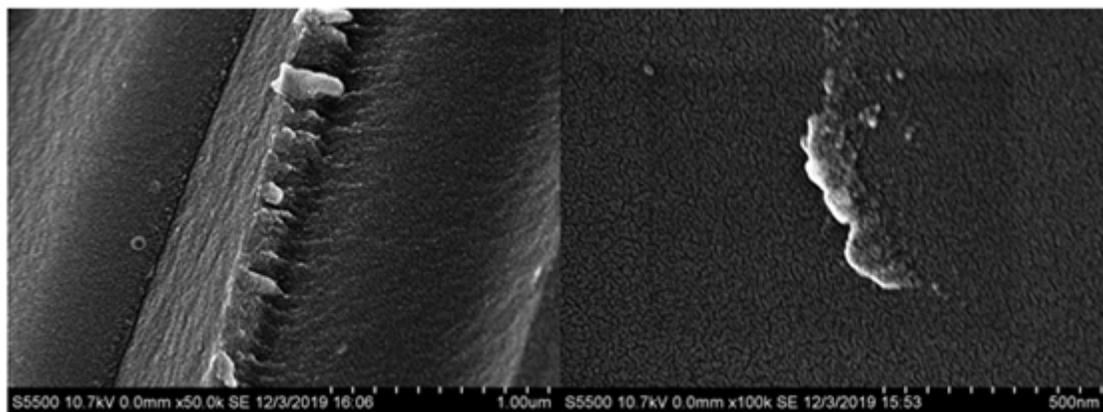


Figure 4

Scanning electron microscopy of the sample 2.1

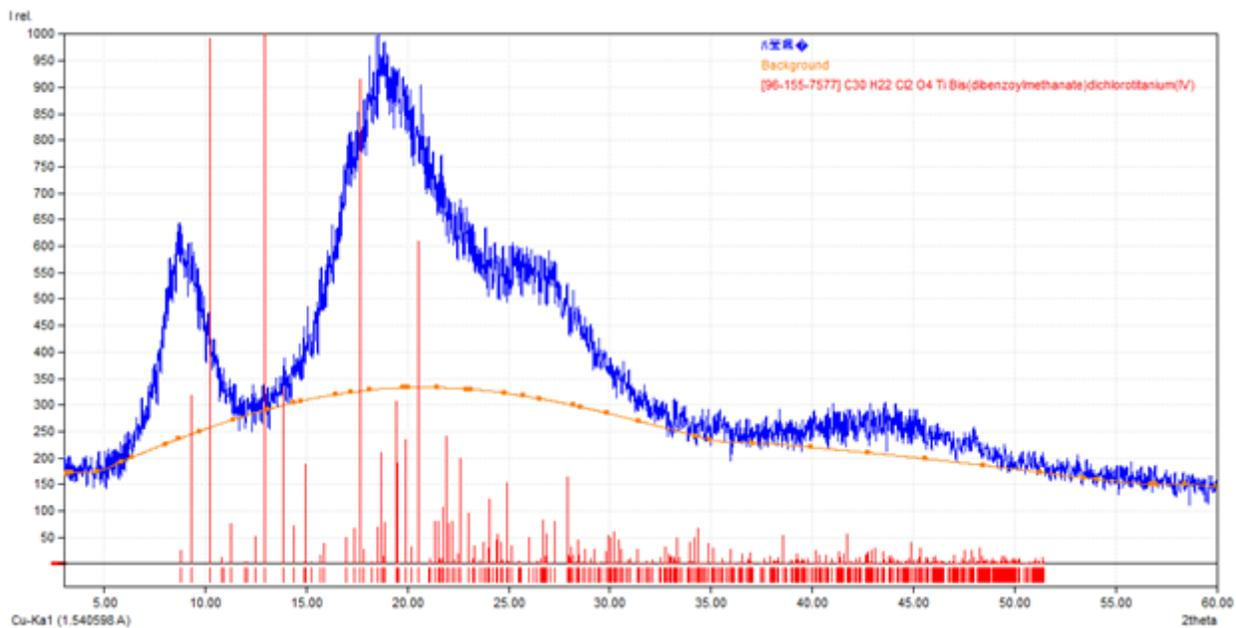


Figure 5

Diffractogram of fraction 2.2

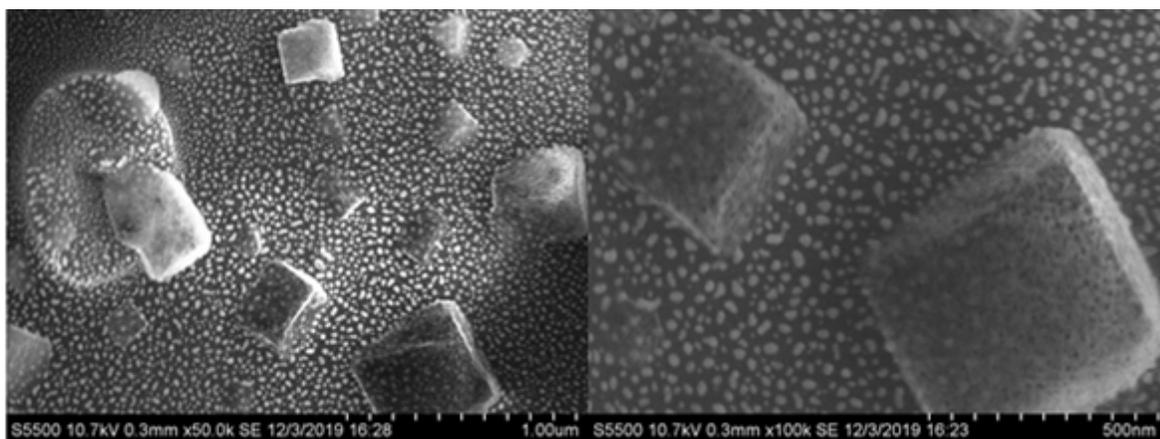


Figure 6

Scanning electron microscopy of the sample 2.2

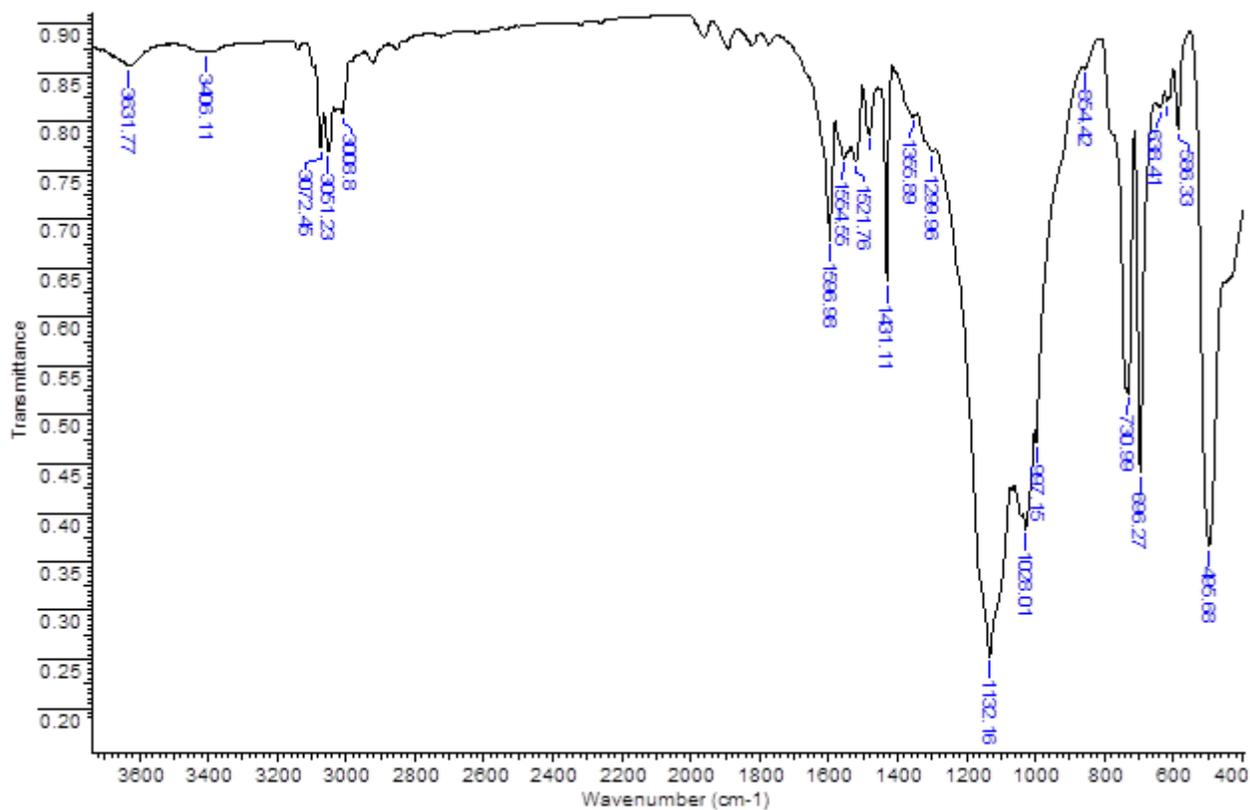


Figure 7

FT-IR spectra of fraction 3.1

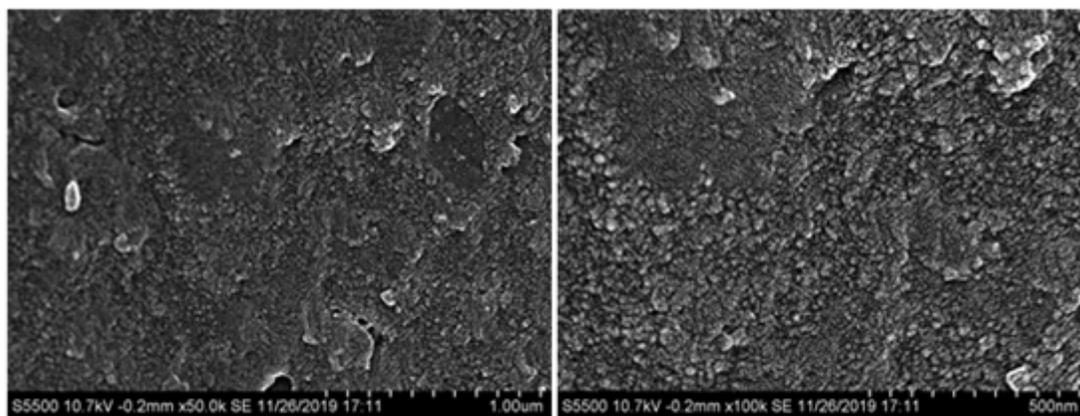


Figure 8

Scanning electron microscopy of the sample 3.1

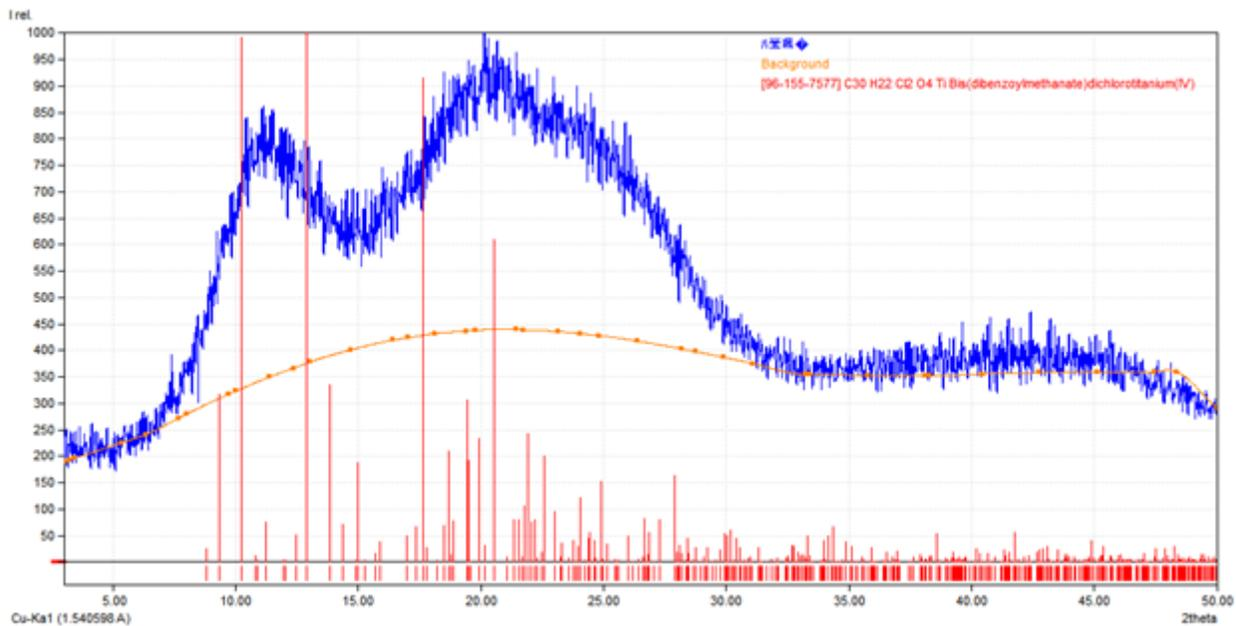


Figure 9

Diffractogram of fraction 3.2

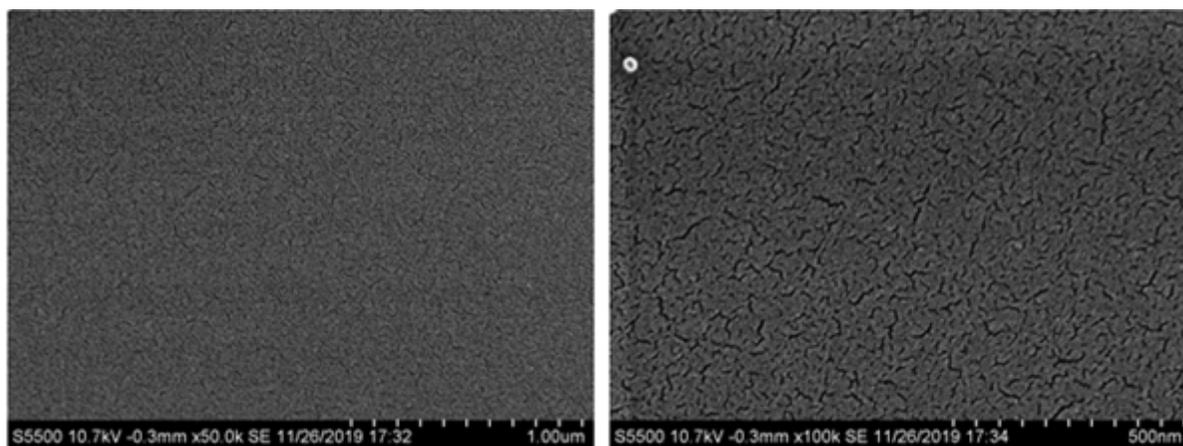


Figure 10

Scanning electron microscopy of the sample 3.2

Supplementary Files

This is a list of supplementary files associated with this preprint. Click to download.

- [supplementarymaterials.docx](#)